Toll-like receptors and inflammation in metabolic neuropathy; a role in early versus late disease?

Elzinga S.E., CO[1], **Murdock B.J., CO**[1], **K. Guo**[2], **J.M. Hayes**[1], **M.A. Tabbey**[1], **J. Hur**[2], **Feldman E.L**[1,*]

[1]Department of Neurology, University of Michigan, Ann Arbor, MI.

[2]Department of Biomedical Sciences, School of Medicine and Health Sciences, University of North Dakota, Grand Forks, ND 58202, USA

Abstract

Neuropathy is a common, morbid complication of the metabolic syndrome, prediabetes, and diabetes. Recent studies have indicated a potential role for the immune system in the development of neuropathy. In particular, toll-like receptors (TLR) 2 and 4 have been linked to metabolic dysfunction, and blocking TLR4 is proposed as a treatment for neuropathic pain. In the current study, we investigated the role of the immune system, particularly TLRs 2 and 4, in the pathogenesis and progression of neuropathy. Sural or sciatic nerve gene expression arrays from humans and murine neuropathy models of prediabetes and diabetes were first analyzed to identify differentially expressed TLR2- and TLR4-associated genes within the KEGG (Kyoto Encyclopedia of Genes and Genomes) database. We observed that genes associated with TLRs 2 and 4, particularly lipopolysaccharide binding protein (*LPB*) and phosphatidylinositol-4,5-bisphosphate 3-kinase catalytic subunit beta (*PIK3CB*), were dysregulated across species and across multiple murine models of prediabetic and diabetic neuropathy. To further understand the role of these pathways *in vivo,* TLR 2 and 4 global knockout mice placed on a 60% high fat diet (HFD-TLR2/4$^{-/-}$) were compared with wild type (WT) mice on a high fat diet (HFD-WT) and WT controls on a standard diet (CON). Mice then underwent metabolic, neuropathic, and immunological phenotyping at two time points to assess the impact of TLR signaling on neuropathy and immunity during metabolic dysfunction over time. We found that HFD-TLR2/4$^{-/-}$ and HFD-WT mice weighed more than CON mice but did not have increased fasting blood glucose levels. Despite normal blood glucose levels, HFD-TLR2/4$^{-/-}$ mice eventually developed neuropathy at the later time point (28 wks of age) but were somewhat protected from neuropathy at the early time point (16 wks of age) as measured by shorter hind paw withdraw latencies. This is in contrast to HFD-WT mice which developed neuropathy within 11 wks of being placed on a high fat diet and were neuropathic by all measures at both the early and late time points. Finally, we immunophenotyped all three mouse groups at the later time point and found differences in the number of peripheral blood Ly6C-myeloid cells as well as F4/80+ expression. These results

*Corresponding author; efeldman@med.umich.edu, Department of Neurology, University of Michigan, 109 Zina Pitcher Place, Ann Arbor, MI, 48109.

indicate that TLR signaling influences early development of neuropathy in sensory neurons, potentially via immune modulation and recruitment.

Keywords

peripheral neuropathy; toll-like receptor 2 and 4; high fat diet

Introduction

Obesity and metabolic dysfunction – in particular the metabolic syndrome, prediabetes, and diabetes – continue to increase in prevalence in the United States and around the world (Ogden et al., 2014; Ogurtsova et al., 2017). The most common sequela of these disorders is neuropathy, which is a major source of patient morbidity and mortality (Callaghan et al., 2012a; Callaghan et al., 2012b; Callaghan et al., 2012c; Callaghan et al., 2016a; Callaghan et al., 2016b). Neuropathy results in an increasing loss of nerve function in a distal to proximal manner, typically progressing in a 'stocking and glove' pattern (Pop-Busui et al., 2017), and despite ongoing research the underlying mechanisms of neuropathy in the context of global metabolic dysfunction are poorly understood.

Immune system dysregulation and low levels of systemic inflammation are both associated with obesity and contribute to the progression of metabolic dysfunction (Arkan et al., 2005; Esser et al., 2014; Jung and Choi, 2014). They have also been proposed as contributors to neuropathy progression (Zeng et al., 2018; Zhang et al., 2018). Using gene profiling and pathway analysis, we recently demonstrated that inflammatory pathways are altered in nervous tissue at multiple time points during metabolic dysregulation (Hinder et al., 2018). Some of the most promising pathways involve pattern recognition toll-like receptors (TLRs), several of which have been linked to obesity and metabolic dysfunction (Dasu et al., 2010; Jia et al., 2014; Reyna et al., 2008). TLRs 2 and 4 are of particular interest (Dasu et al., 2010; Song et al., 2006), and both TLRs 2 and 4 can be activated by free fatty acids, which are commonly elevated in obesity and metabolic dysfunction (Fessler et al., 2009; Lee et al., 2004). TLR activation in response to fatty acids can result in perturbations in the insulin signaling pathway, including induction of phosphorylation and subsequent inactivation of insulin receptor substrate-1 (Hotamisligil et al., 1996; Zhang et al., 2016), and knocking out either TLR2 or TLR4 results in protection from insulin resistance despite ingestion of a high fat diet (HFD) (Davis et al., 2011; Davis et al., 2008; Lumeng, 2013; Shi et al., 2006). Knockout (KO) or knockdown of TLR4 in mice improves mechanical sensitivity, thermal sensitivity, and pain in neuropathy models, and reduces inflammation or immune cell infiltration in spinal cord or dorsal root ganglion neurons (Bettoni et al., 2008; Liu et al., 2016; Wu et al., 2010). Additionally, TLR4 gene expression in peripheral blood is increased in human type 2 diabetic patients and further increased in type 2 diabetic patients with neuropathy, and along with circulating tumor necrosis factor alpha (TNF-α) concentrations, had a high and significant adjusted odds ratio for neuropathy above that of body mass index and hemoglobin A1c (Zhu et al., 2015).

In the current study, we further explored the role of TLRs in neuropathy by comparing available sural and sciatic nerve gene expression profiles from humans with diabetic neuropathy and from multiple murine models of prediabetic and diabetic neuropathy. In parallel, we utilized a well-established paradigm of high fat feeding to induce neuropathy in a TLR 2 and 4 global KO mouse model (TLR2/4$^{-/-}$) to assess the role of TLR signaling in the onset and progression of neuropathy at early and late time points. Finally, TLR2/4$^{-/-}$ mice fed a HFD were immunophenotyped to identify immune system changes that may play a role in neuropathy development and progression.

Materials and Methods

Post-hoc gene expression comparison

Human microarray gene expression data (Hur et al., 2011) were assessed in diabetic patients who either progressed in their neuropathy (progressors) or did not progress in neuropathy (non-progressors) as measured by changes in sural nerve myelin fiber density over a period of 52 wks. Sural nerve differentially expressed genes (DEGs) were obtained from two studies using different analysis platforms: ChipInspector (Genomatix Software GmbH) allowing single probe-level analysis (McGregor et al., 2018), and GenePattern using the standard robust multi-array average-based probe set approach combined with ChipInspector (Hur et al., 2011). DEG datasets from murine models were obtained from multiple published datasets by comparing diabetic to healthy control mice or by comparing diabetic mice across different time points. The murine datasets included sciatic nerve gene expression data from: 1) 8 and 24 wk old *db/db* type 2 diabetic mice compared over time or compared to *db/+* non-diabetic controls (Hinder et al., 2018; Pande et al., 2011), 2) 26 wk old DBA/2J low dose streptozotocin (STZ)-induced type 1 diabetic mice compared to DBA/2J non-diabetic mice not given STZ (Wiggin et al., 2008), 3) 16 wk old *db/db* mice treated with the peroxisome proliferator-activated receptor gamma agonist, pioglitazone, compared to untreated *db/db* mice or to *db/+* non-diabetic controls (Hur et al., 2015), 4) 5 and 13 wk old male BTBR *ob/ob* type 2 diabetic mice compared over time or compared to *ob/+* non-diabetic control mice (O'Brien et al., 2015), 5) 26 wk old female BTBR *ob/ob* type 2 diabetic mice compared to *ob/+* non-diabetic controls (O'Brien et al., 2016), and 6) a second cohort of 16 wk *db/db* mice treated with pioglitazone compared to untreated *db/db* mice or to *db/+* non-diabetic controls (Hinder et al., 2017b). DEGs from these human and murine datasets were compiled and cross-referenced against the genes in the KEGG (Kyoto Encyclopedia of Genes and Genomes) TLR signaling pathways (https://www.genome.jp/kegg-bin/show_pathway?map04620).

Murine studies and metabolic phenotyping

Ten C57BL/6J mice and 5 TLR2/4$^{-/-}$ mice of the same strain were obtained. Of the non-genetically modified animals, 5 were utilized as controls (CON; 3 males and 2 females) and received standard chow, whereas the remaining 5 were placed on a HFD (HFD-WT; 2 males and 3 females). TLR2/4$^{-/-}$ mice were switched to a 60% HFD at 5 wks of age (HFD-TLR2/4$^{-/-}$; 2 males and 3 females). Metabolic and neuropathic phenotyping was performed at an early time point (16 wks of age) and at a later time point (28 wks of age), with additional immunophenotyping completed at 28 wks. Body weights and fasting (4 hr) blood

glucose measured using an AlphaTrak Glucometer (Abbott Laboratories, Abbott Park, IL, USA) were recorded weekly.

Neuropathy phenotyping

Animals were phenotyped for neuropathy at 16 and 28 wks of age using the Animal Models of Diabetic Complications Consortium guidelines (Biessels et al., 2014). Specifically, we measured sural sensory (sural NCV) and sciatic motor (SMNCV) nerve conduction velocities (NCVs), hind paw withdrawal latencies (HPLs), and intraepidermal nerve fiber densities (IENFDs). NCV was measured per our previous publications (Oh et al., 2010; Stevens et al., 1994). In brief, we measured sural NCV by applying an antidromic stimulus at the ankle and recording at the dorsum of the foot. Onset latency of the action potential and distance were measured and the NCV calculated. For SMNCV, orthodromic stimulation was applied at the ankle, followed by the sciatic notch, and recorded at the dorsum of the foot for each stimulus. The onset latency of the action potential and distance for each component was measured. The ankle latency was subtracted from the notch latency, and ankle distance was subtracted from the notch distance. The resultant latency and distance were used to measure conduction velocity. NCVs are presented as meters per second (m/s).

HPLs were measured as previously described (Lee et al., 1990; Sullivan et al., 2007). In brief, mice were confined to an acrylic box on top of a 32°C heated glass plate. A red-light emitter (60-170°C) was used under the hind paw and incrementally increased from 25° - 70°C. The time it took for the hind paw to withdraw from the heat stimulus was used to determine HPL. HPLs are presented as seconds (s) (Lee et al., 1990).

IENFDs were assessed at the terminal time point using previously published protocols (Cheng et al., 2012; Sullivan et al., 2007). In brief, hind paw footpads were fixed 4-6 hr in Zamboni's fixative (Newcomer Supply, Middleton, WI, USA), then sectioned at 30 μm. Floating sections were stained with protein gene product 9.5 (PGP9.5; cat. no. 14730-1-AP, Proteintech, Rosemont, IL, USA) and labeled with Alexa Fluor 488 (cat. no. A-11034, ThermoFisher, Waltham, MA, USA). Sections were counterstained and mounted to slides using prolong gold with dapi (cat. no. P36931, ThermoFisher, Waltham, MA, USA). For each mouse, we captured 4 z-series images and the total distance counted was at least 3 mm. Images were taken with a confocal microscope (Olympus Fluoview 500, 20× air objective, 1024×1024 pixel resolution; Shinjuku, Tokyo, Japan). Z-series were converted to max project images and the number of nerve fibers innervating the epidermis were counted using MetaMorph software (v.7.7.0.8, Molecular Devices, Sunnyvale, CA, USA).

Immunologic phenotyping

At the terminal endpoint of the study (28 wks) circulating immune cells were isolated from peripheral blood and immunophenotyped using flow cytometry (Murdock et al., 2012). In brief, lymphoid and myeloid leukocytes were characterized using a battery of fluorescently labeled antibodies specific for well-characterized leukocyte surface markers. Forward scatter width and height were first used to exclude doublets, and APC-CD45was then used to identify leukocytes. Lymphoid cells were identified by excluding side scatter (SSC)-high cells and identifying lymphocytes (APC-Cy7-CD4+ or BV421-CD8+ cells) within the

FITC-CD3+ fraction. Natural killer (NK) cells (PE-NK1.1+) and B cells (PerCp-5.5-CD19+) were identified within the CD3− fraction. In the myeloid stain, CD45+ leukocytes were first separated by SSC expression; neutrophils were identified as SSC-high PE-Cy7-Ly6G+ cells. Within the SSC-low fraction, monocyte populations were APC-Cy7-CD11b+, and these populations were classified as either Ly6C− or Ly6C+ based on their expression of FITC-Ly6C. Within the two monocyte populations, F4/80 expression levels were assessed using the median fluorescent intensity (MFI) of PE-F4/80. All antibodies were purchased from Biolegend (San Diego, CA), samples were run using a FACSAria II (BD Biosciences, San Jose, CA, USA), and data were analyzed using FlowJo software (FlowJo, Ashland, OR, USA).

Statistical analysis

For analysis of neuropathy across multiple time points, statistical analysis was performed using SAS version 9.4 (SAS institute, Carry, NC, USA) with the PROC mixed function. Group and gender and their interaction were set as main effects and were tested against each variable. Normality was assessed using the Kolmogorov-Smirnov test; non-normal data were log transformed to achieve normality. For peripheral blood immune levels, statistical analysis was performed using GraphPad Prism 7.0 (GraphPad Software, Inc., La Jolla, CA, USA) using oneway analysis of variance (ANOVA) followed by Tukey's multiple comparisons. Statistical significance was defined as $P < 0.05$ and trends considered at $P < 0.10$.

Results

Post-hoc gene expression analysis

We have previously demonstrated increased inflammatory gene expression in peripheral nerves in human tissue and in multiple mouse models of diabetic neuropathy (Hinder et al., 2018; Hinder et al., 2017b; Hur et al., 2011; Pande et al., 2011). To assess which specific inflammatory mechanisms may be playing a role in disease, we analyzed our pre-existing data sets and compared sural and sciatic nerve gene expression patterns across both man and murine models of both type 1 and 2 diabetes. Specifically, we looked for changes in TLR 2 and 4 signaling pathways, as these receptors have been previously linked to altered metabolism, neuropathy, and neuropathic pain (Bettoni et al., 2008; Dasu et al., 2010; Davis et al., 2011; Liu et al., 2016).

In human tissue, we compared gene expression between two groups: human diabetic patients with neuropathy that progressed (progressors) and diabetic patients with neuropathy that did not progress over a period of 52 wks (non-progressors). KEGG pathway analysis was used to identify DEGs associated with TLR signaling. Using the ChipInspector (Genomatix Software GmbH) analysis platform, we identified 27 sural nerve TLR DEGs (Table 1). These genes included numerous MAP kinases, phosphoinositide kinases, and numerous adaptor proteins and transcription factors. In addition, cytokines and chemokines have been implicated in obesity, diabetes, and neuropathy (Doupis et al., 2009; Esser et al., 2014), and both chemokine (C-X-C motif) ligand 9 (*CXCL9*) and ligand 11 (*CXCL11*) were significantly downregulated in our analysis. To further refine our pathway analysis, we

investigated the 27 DEGs using Genepattern software in conjunction with ChipInspector. Of the initial 27 DEGs, 4 were dysregulated across both analysis platforms. These four genes included jun proto-oncogene (*JUN*), lipopolysaccharide binding protein (*LBP*), phosphoinositide-3-kinase (catalytic) beta polypeptide (*PIK3CB*), and TLR adaptor molecule 1 (*TICAMI*).

In parallel, we examined gene expression changes associated with TLR pathways across multiple mouse models of metabolic dysfunction from previously published data sets. These models included *db/db* mice (Hinder et al., 2018; Pande et al., 2011), DBA/2J streptozotocin (STZ)-induced type 1 diabetic mice (Wiggin et al., 2008), *db/db* mice treated with pioglitazone, and *ob/ob* mice (O'Brien et al., 2015; O'Brien et al., 2016). Several of these models were analyzed at multiple time points (Hinder et al., 2017b; Hur et al., 2015; O'Brien et al., 2015; O'Brien et al., 2016). Using murine KEGG TLR 2 and 4 pathway data, we identified a total of 55 DEGs (Table 2). Canonically, TLR 2 and 4 signal though the Myeloid Differentiation Primary Response 88 (MyD88) pathway (Lu et al., 2008), and gene expression within this pathway, was dysregulated for multiple genes. Expression of *Tlr2* itself was upregulated at 5 wks of age in *ob/ob* mice compared to controls but decreased from 5 to 13 wks of age in that same type 2 diabetic model. *Tlr4* expression was not significantly different in any of the murine comparisons, but expression of adapter proteins within the TLR4 complex (*Cd14* and *Lbp*) were altered across multiple data sets. Similar to human tissue samples, we also observed changes in cytokine and chemokine gene expression patterns. Of note, *TNFa* and interleukin 1 beta (*IL-1β*), two cytokines often associated with obesity and metabolic dysfunction, were dysregulated in multiple data sets, and both were upregulated early in *ob/ob* mice.

Similar to our analysis of human tissue, we further refined our analysis of murine DEGs by examining overlapping gene expression patterns. Here, we analyzed DEGs from all the mouse model data sets simultaneously and looked for genes that were dysregulated across multiple data sets. Of the initial 55 TLR-related murine DEGs, there were 7 DEGs that were dysregulated across 4 or more murine models. These seven DEGs included thymoma viral proto-oncogene 3 (*Akt3*), chemokine (C-C motif) ligand 3 (*Ccl3*), *Lbp, Pik3cb*, phosphatidylinositol-3-kinase (regulatory subunit 5, p101; *Pik3r5*), secreted phosphoprotein 1 (*Spp1*), and TGF-beta activated kinase 1/MAP3K7 binding protein 1 (*Tab1*).

As a final step, we compared DEGs across species, looking for pathways that were dysregulated in both human and mouse neuronal tissue. Of the 27 human DEGs, 20 (74%) were also dysregulated in at least one murine model, and 2 DEGs (*LBP* and *PIK3CB*) were found in the more stringent analyses for both the human and mouse data sets (Table 3). To further our analysis, we also examined the directionality of gene expression changes in humans and mice. Human DEGs could either be upregulated or downregulated, while mouse DEG expression could be upregulated, downregulated, or mixed (up- or downregulated dependent on mouse model). Of the 20 overlapping DEGs, 5 had mixed responses in mice (*AKT2, CD86, CXCL9, LBP, MAP2K7*), meaning there was neither concordance nor discordance in the directionality of human and mouse gene expression. Of the remaining 15 DEGs, only 2 (*MAPK10* and *STAT1*) showed concordance between human and murine dysregulated gene expression, while 13 of the 15 DEGs (87%) were discordant. However,

directionality of gene expression in murine data sets often differed dependent upon time point, treatment, or strain. Together, these data indicate that similar TLR pathways are dysregulated in human and murine nervous tissue, but the directionality of gene expression is affected by multiple factors, including time, strain, and species.

Metabolic phenotyping

Having observed changes in TLR-associated genes in human and murine data sets, we extended our analyses to an *in vivo* model system. To do so, we took TLR2/4$^{-/-}$ mice and placed them on a HFD (HFD-TLR2/4$^{-/-}$) for 23 wks in order to assess the impact of TLR loss on the development of neuropathy. We began by comparing metabolic changes in HFD-TLR2/4$^{-/-}$ and WT mice placed on a HFD (HFD-WT) with WT control mice (CON) on a standard diet. Consistent with our previous studies (Hinder et al., 2017a; O'Brien et al., 2018), both strains of mice placed on a HFD gained weight over the course of the study (Table 4). In both HFD-WT and HFD-TLR2/4$^{-/-}$ mice, there was a trend towards increased fasting blood glucose levels, but these numbers did not reach statistical significance. Together, these data indicate that HFD-TLR2/4$^{-/-}$ mice develop increased obesity in response to a HFD without significantly altered fasting blood glucose levels. Thus, any differences observed in neuropathy were hyperglycemia independent in HFD-WT and HFD-TLR2/4$^{-/-}$ mice.

Neuropathy phenotyping

We next tested whether deletion of the TLR2 and TLR4 genes would alter the development of neuropathy. First, we measured NCVs of CON, HFD-WT, and HFD-TLR2/4$^{-/-}$ mice at an early time point (16 wks of age) and a late time point (28 wks of age). Consistent with our previous reports (Hinder et al., 2017a), mice fed a HFD had reduced NCVs in both the sural nerve (Fig. 1A) and sciatic-tibial motor nerve (Fig. 1B) at both the early and the late time points. HFD-TLR2/4$^{-/-}$ likewise had reduced NCVs compared to CON; however, sural NCVs worsened from the 16- to the 28-wk time points. These temporal differences were not observed in SMNCV, which displayed significant NCV deficits in both HFD-WT and HFD-TLR2/4$^{-/-}$ mice regardless of time point.

To support these observations, we next assessed HPLs in all three mouse groups at both the early and late time points. As previously reported (Obrosova et al., 2007), HFD-WT mice had increased thermal latency, indicating a loss of sensation in the paw (Fig. 1C). These deficits were observed at both the early and the late time points. In contrast, HFD-TLR2/4$^{-/-}$ mice were protected from this loss of sensation at the early time point: there was no significant difference in HPL in HFD-TLR2/4$^{-/-}$ mice at 16 wks of age compared to CON. However, as with sural NCV, by 28 wks HFD-TLR2/4$^{-/-}$ HPL had significantly increased in these KO animals compared to the earlier time point. Additionally, they were no longer similar to CON and were similar to HFD-WT mice.

As a final assessment of TLR impact on neuropathy, we measured IENFDs of all three mouse groups at 28 wks of age (Fig. 1D; Supplemental Fig. 1). HFD-WT had significantly reduced IENFD compared to CON mice. IENFDs in HFD-TLR2/4$^{-/-}$ mice did not have a significant deficit relative to CON; however, they were likewise not different from HFD-WT

mice. Together, these data indicate that blocking TLR2/4 protects sensory nerves during early neuropathy, but this protection is lost over time. The data also suggest that TLR contribution to neuropathy may be more prominent in sensory nerves, as the sciatic-tibial motor NCVs were unaffected by the gene KOs.

Immunologic phenotyping

To further understand the role of TLR signaling on the development of neuropathy, we measured immunologic changes in the peripheral blood of CON, HFD-WT, and HFD-TLR2/4$^{-/-}$ mice following their harvest at 28 wks of age. Total leukocyte counts, as well as numbers of specific immune populations, were assessed using flow cytometry (Fig. 2A). Consistent with previous reports (Fink et al., 2014), HFD-WT mice displayed increased numbers of peripheral immune cells compared to CON mice; this was partially reversed in HFD-TLR2/4$^{-/-}$ mice. A similar pattern was observed in the number of neutrophils and Ly6C+ myeloid cells in the peripheral blood, with significantly increased neutrophil levels in HFD-WT mice and a trend towards reduced numbers in HFD-TLR2/4$^{-/-}$ mice in both cell types. CD4 T cell, CD8 T cell, and Ly6C-myeloid cell levels were not significantly altered by a HFD or lack of TLR signaling. Interestingly, we observed a significant reduction in NK cell levels in the peripheral blood of HFD-TLR2/4$^{-/-}$ mice compared to HFD-WT mice, and the significant increase in B cells observed in HFD-WT mice was completely reversed by TLR 2/4 KO.

In addition to total cell numbers, we used flow cytometry to examine classical surface marker expression levels for monocyte populations in peripheral blood. We found that Ly6C − and Ly6C+ monocytes did not express CD11c on the cell surface in any mouse group (data not shown), indicating that a HFD did not inducing monocyte differentiation into macrophages or dendritic cells in the periphery (Gower et al., 2011; Strauss-Ayali et al., 2007). In contrast, F4/80, a marker found primarily on monocytes and differentiated macrophages (Hirsch et al., 1981), was dramatically upregulated on the surface of both Ly6C− and Ly6C+ monocytes in HFD-TLR2/4$^{-/-}$ mice compared to CON and HFD-WT mice (Fig. 2B). Together, these data indicate that a lack of TLR 2 and 4 signaling reduces HFD-induced peripheral inflammation, and that a lack of TLR signaling fundamentally alters the phenotype of myeloid cells in the periphery during high fat feeding.

Discussion

Low-grade systemic inflammation and immune system dysregulation are common features of prediabetes, diabetes, and peripheral neuropathy (Esser et al., 2014; Hinder et al., 2018). TLR signaling, particularly signaling via TLR 2 and 4, are implicated in the pathogenesis and progression of metabolic disease states (Lumeng, 2013). In the current study, we explored the role of TLR2/4 and TLR-associated pathways during metabolic dysregulation, as well as the impact of TLRs on the development of neuropathy and peripheral inflammation. We examined TLR 2/4 pathway gene expression levels in both human nerves and in nerves from murine models of prediabetes, type 1 diabetes, and type 2 diabetes and found that TLR 2 and 4 signaling is dysregulated in human patients and across murine models. The majority of these changes were conserved between human and murine samples,

but gene expression patterns were variable based on time point, strain, treatment, and species. We next examined the impact of TLR2/4 KO on the development of neuropathy. While TLR2/4 KO resulted in increased obesity in HFD-TLR2/4$^{-/-}$ mice compared to HFD-WT mice, HFD-TLR2/4$^{-/-}$ mice were partially protected from neuropathy during an early time point. In addition, we found that knocking out TLR2 and TLR4 reduced the peripheral inflammation induced by a HFD, resulting in fewer immune cells but increased F4/80 expression on two populations of monocytes.

Our initial *post-hoc* comparisons of sural nerve gene expression showed that TLR-associated genes are dysregulated both in human and murine neuropathy in prediabetes and diabetes. Of note, we observed dysregulation of *LBP* and *PIK3CB* in human data sets and across 4 or more murine data sets. The involvement of *LBP* is perhaps unsurprising, as it is part of the canonical TLR4 signaling pathway and facilitates presentation of TLR4's primary ligand, lipopolysaccharide, to the TLR4 receptor complex (Kim and Kim, 2017). *PIK3CB*, on the other hand, is a member of the phosphoinositide 3-kinase (PI3K) family which has multiple roles in cellular function, including cell growth and survival (Engelman et al., 2006), and class I PI3Ks, including *PIK3CB*, are involved in insulin and AKT signaling (Engelman et al., 2006; Le Stunff et al., 2008). These signaling pathways have been implicated in insulin resistance (Le Stunff et al., 2008), inflammation in sensory neurons (Zhuang et al., 2004), and neuropathy and neuropathic pain (Duan et al., 2018; Yang et al., 2014). While PI3Ks can be activated through multiple mechanisms, TLRs and co-stimulatory molecules are major sources of their activation (Koyasu, 2003) and likely explain why these genes were dysregulated during neuropathy in both human and murine nervous tissue.

Interestingly, while there was a great deal of overlap between dysregulated human and murine genes, the direction in which these genes changed was often different between the species. Differences in the directionality of human versus murine gene expression may be partly explained by different neuropathy time points as well as genetic differences between phenotypically different mouse strains (O'Brien et al., 2014; Sullivan et al., 2007). For instance, the *ob/ob* type 2 diabetes mouse strain, which develops the most robust neuropathy phenotype (O'Brien et al., 2015), had numerous TLR genes that were discordant between 5 and 13 wks of age, including *Ccl3, Ccl4, Cd14, Cd86, Il1b,* and *Tlr2.* This discordance indicates that TLR gene expression in this model associates with neuropathy progression. In addition, we have previously reported that numerous genes, including inflammatory genes, can be differentially regulated over the course of neuropathy (Hinder et al., 2018). The possibility that TLR involvement in neuropathy is time dependent is bolstered by our *in vivo* data where TLR KO was protective at the early time point but not at the later time point. In addition, the human tissue samples were collected from patients that had been living with diabetes for an average of 10 years (Hur et al., 2011); the DEGs that were highlighted in our analysis likely represent a late stage of neuropathy development. Changes in directionality of gene expression therefore reflect a complex interaction between time, the inflammatory response, and disease progression.

This temporal nature of TLR involvement in neuropathy may partially explain why sural nerve function worsened from the early to late time points in HFD-TLR2/4$^{-/-}$ mice. Additionally, HPL was significantly better at 16 wks of age in HFD-TLR2/4$^{-/-}$ mice

compared to HFD-WT mice and was similar to CON. However, like sural NCVs, this worsened over time in HFD-TLR2/4$^{-/-}$ mice, with latencies similar to HFD-WT mice at 28 wks of age. IENFD at 28 wks of age suggested a "lingering" protective effect in HFD-TLR2/4$^{-/-}$ mice despite worsened NCVs and HPLs at this time point. In contrast to the findings in sensory nerves, there was no early protective effect of lack of TLR signaling on SMNCVs at 16 wks of age. Peripheral neuropathy, in particular peripheral neuropathy driven by HFD, has a larger effect early in disease on sensory as opposed to motor nerves, and first affects small unmyelinated axons (Feldman et al., 2017). Changes in HPL and IENFD in these data similarly indicate a predominant effect at earlier time points on sensory unmyelinated nerve fibers. We also observed changes in myelinated sensory nerve fibers as evidenced by the changes is sural NCVs. Altogether, these data suggest that TLR involvement in neuropathy, particularly at earlier time points, has a greater impact on sensory nerves with little impact or no impact on motor nerves.

Based on our immune phenotyping data, it is possible that TLR signaling contributes to neuropathy via alterations in immune system signaling. Knocking out TLRs 2 and 4 produced an anti-inflammatory phenotype in the peripheral blood of mice. HFD-WT mice had increased peripheral leukocytes compared to CON mice, but this expansion of inflammatory cells was partially rescued in HFD-TLR2/4$^{-/-}$ mice. There was a trend towards fewer neutrophils and Ly6C+ monocytes in HFD-TLR2/4$^{-/-}$ mice, and the number of NK cells and B cells was significantly reduced. The most striking differences, however, were the surface expression levels of F4/80 on both Ly6C– and Ly6+ monocyte populations. F4/80 expression on HFD-TLR2/4$^{-/-}$ monocytes was significantly increased compared to both CON and HFD-WT monocytes. Though the exact mechanisms and function of F4/80 are still not fully understood, multiple studies suggest that F4/80 has an anti-inflammatory function that can suppress leukocyte activity (Gordon et al., 2011). This suggests that an absence of TLR signaling may skew circulating monocytes towards a protective phenotype that could account for the early protection against neuropathy in HFD-TLR2/4$^{-/-}$ mice. Further studies in a larger cohort of mice may strengthen the observed trends and contribute to fuller mechanistic understanding of the role of TLRs 2 and 4 in neuropathy.

In conclusion, both the *post-hoc* comparisons and *in vivo* data emphasize varying and complex effects of time and TLR signaling on neuropathy progression. In our *post-hoc* comparisons of murine sciatic nerve gene expression in multiple different models of prediabetic and diabetic neuropathy, many genes within the TLR 2/4 pathway were significantly upregulated at earlier disease time points, but decreased with age and increasing disease severity. These data were supported by our findings in the HFD-TLR2/4$^{-/-}$ mice. These animals did not develop neuropathy early in the course of high fat feeding, with HPLs similar to CON mice. However, as disease progressed, HPLs and sural NCVs worsened, and HFD-TLR2/4$^{-/-}$ mice were similar to HFD-WT rather than CON mice. These results are potentially due to an anti-inflammatory phenotype in HFD-TLR2/4$^{-/-}$ mice that protects against damage early on, but as neuropathy progresses the beneficial effects of inflammation are lost (Ramesh et al., 2013), resulting in a lack of clearance of damaged cells and cellular debris and a worsening of dysfunction. Together, our findings suggest that the TLR 2 and 4 pathways play a role in the development of neuropathy, suggesting a role for inflammation in neuropathy secondary to prediabetes and

diabetes. While these data support a role for TLRs in neuropathy, however, gene expression was assessed in whole nerve which is a heterogeneous population of cells. Further studies in larger cohorts will be needed to adjust for cell-type specific contributions as well as to elucidate exact contributing mechanisms and allow for potential future therapeutic development.

Summary

These results support a role for TLRs 2 and 4 in the progression of prediabetic and diabetic sensory neuropathy in both man and multiple murine models. Additionally, our data indicate a delicate balance between the immune response, inflammation, and disease progression. However, more work is needed to fully understand the role of TLRs 2 and 4 in the onset and progression of prediabetic and diabetic neuropathy.

Supplementary Material

Refer to Web version on PubMed Central for supplementary material.

Acknowledgements

References

Arkan MC, Hevener AL, Greten FR, Maeda S, Li Z-W, Long JM, Wynshaw-Boris A, Poli G, Olefsky J, Karin M, 2005 IKK-β links inflammation to obesity-induced insulin resistance. Nature medicine 11, 191.

Bettoni I, Comelli F, Rossini C, Granucci F, Giagnoni G, Peri F, Costa B, 2008 Glial TLR4 receptor as new target to treat neuropathic pain: efficacy of a new receptor antagonist in a model of peripheral nerve injury in mice. Glia 56, 1312–1319. [PubMed: 18615568]

Biessels G, Bril V, Calcutt N, Cameron N, Cotter M, Dobrowsky R, Feldman E, Fernyhough P, Jakobsen J, Malik R, 2014 Phenotyping animal models of diabetic neuropathy: a consensus statement of the diabetic neuropathy study group of the EASD (Neurodiab). Journal of the Peripheral Nervous System 19, 77–87. [PubMed: 24934510]

Callaghan BC, Cheng HT, Stables CL, Smith AL, Feldman EL, 2012a Diabetic neuropathy: clinical manifestations and current treatments. The Lancet Neurology 11, 521–534. [PubMed: 22608666]

Callaghan BC, Hur J, Feldman EL, 2012b Diabetic neuropathy: one disease or two? Current opinion in neurology 25, 536. [PubMed: 22892951]

Callaghan BC, Little AA, Feldman EL, Hughes RA, 2012c Enhanced glucose control for preventing and treating diabetic neuropathy. The Cochrane Library.

Callaghan BC, Xia R, Banerjee M, de Rekeneire N, Harris TB, Newman AB, Satterfield S, Schwartz AV, Vinik AI, Feldman EL, 2016a Metabolic syndrome components are associated with symptomatic polyneuropathy independent of glycemic status. Diabetes care, dc160081.

Callaghan BC, Xia R, Reynolds E, Banerjee M, Rothberg AE, Burant CF, Villegas-Umana E, Pop-Busui R, Feldman EL, 2016b Association Between Metabolic Syndrome Components and Polyneuropathy in an Obese Population. JAMA Neurol 73, 1468–1476. [PubMed: 27802497]

Cheng HT, Dauch JR, Hayes JM, Yanik BM, Feldman EL, 2012 Nerve growth factor/p38 signaling increases intraepidermal nerve fiber densities in painful neuropathy of type 2 diabetes. Neurobiology of disease 45, 280–287. [PubMed: 21872660]

Dasu MR, Devaraj S, Park S, Jialal I, 2010 Increased toll-like receptor activation and TLR ligands in recently diagnosed type 2 diabetes subjects. Diabetes care.

Davis JE, Braucher DR, Walker-Daniels J, Spurlock ME, 2011 Absence of Tlr2 protects against high-fat diet-induced inflammation and results in greater insulin-stimulated glucose transport in cultured adipocytes. The Journal of nutritional biochemistry 22, 136–141. [PubMed: 20434320]

Davis JE, Gabler NK, Walker-Daniels J, Spurlock ME, 2008 Tlr-4 deficiency selectively protects against obesity induced by diets high in saturated fat. Obesity 16, 1248–1255. [PubMed: 18421279]

Doupis J, Lyons TE, Wu S, Gnardellis C, Dinh T, Veves A, 2009 Microvascular reactivity and inflammatory cytokines in painful and painless peripheral diabetic neuropathy. The Journal of Clinical Endocrinology & Metabolism 94, 2157–2163. [PubMed: 19276232]

Duan Z, Su Z, Wang H, Pang X, 2018 Involvement of pro-inflammation signal pathway in inhibitory effects of rapamycin on oxaliplatin-induced neuropathic pain. Molecular pain 14, 1744806918769426. [PubMed: 29587559]

Engelman JA, Luo J, Cantley LC, 2006 The evolution of phosphatidylinositol 3-kinases as regulators of growth and metabolism. Nature Reviews Genetics 7, 606.

Esser N, Legrand-Poels S, Piette J, Scheen AJ, Paquot N, 2014 Inflammation as a link between obesity, metabolic syndrome and type 2 diabetes. Diabetes research and clinical practice 105, 141–150. [PubMed: 24798950]

Feldman EL, Nave K-A, Jensen TS, Bennett DL, 2017 New horizons in diabetic neuropathy: Mechanisms, bioenergetics, and pain. Neuron 93, 1296–1313. [PubMed: 28334605]

Fessler MB, Rudel LL, Brown M, 2009 Toll-like receptor signaling links dietary fatty acids to the metabolic syndrome. Current opinion in lipidology 20, 379. [PubMed: 19625959]

Fink LN, Costford SR, Lee YS, Jensen TE, Bilan PJ, Oberbach A, Blüher M, Olefsky JM, Sams A, Klip A, 2014 Pro-inflammatory macrophages increase in skeletal muscle of high fat-fed mice and correlate with metabolic risk markers in humans. Obesity 22, 747–757. [PubMed: 24030890]

Gordon S, Hamann J, Lin HH, Stacey M, 2011 F4/80 and the related adhesion-GPCRs. European journal of immunology 41, 2472–2476. [PubMed: 21952799]

Gower RM, Wu H, Foster GA, Devaraj S, Jialal I, Ballantyne CM, Knowlton AA, Simon SI, 2011 CD11c/CD18 expression is upregulated on blood monocytes during hypertriglyceridemia and enhances adhesion to vascular cell adhesion molecule-1. Arteriosclerosis, thrombosis, and vascular biology 31, 160–166.

Hinder LM, Murdock BJ, Park M, Bender DE, O'Brien PD, Rumora AE, Hur J, Feldman EL, 2018 Transcriptional networks of progressive diabetic peripheral neuropathy in the db/db mouse model of type 2 diabetes: An inflammatory story. Experimental neurology 305, 33–43. [PubMed: 29550371]

Hinder LM, O'Brien PD, Hayes JM, Backus C, Solway AP, Sims-Robinson C, Feldman EL, 2017a Dietary reversal of neuropathy in a murine model of prediabetes and metabolic syndrome. Dis Model Mech 10, 717–725. [PubMed: 28381495]

Hinder LM, Park M, Rumora AE, Hur J, Eichinger F, Pennathur S, Kretzler M, Brosius FC, Feldman EL, 2017b Comparative RNA-Seq transcriptome analyses reveal distinct metabolic pathways in diabetic nerve and kidney disease. Journal of Cellular and Molecular Medicine.

Hirsch S, Austyn J, Gordon S, 1981 Expression of the macrophage-specific antigen F4/80 during differentiation of mouse bone marrow cells in culture. Journal of Experimental Medicine 154, 713–725. [PubMed: 7276827]

Hotamisligil GS, Peraldi P, Budavari A, Ellis R, White MF, Spiegelman BM, 1996 IRS-1-mediated inhibition of insulin receptor tyrosine kinase activity in TNF-α-and obesity-induced insulin resistance. Science 271, 665–670. [PubMed: 8571133]

Hur J, Dauch JR, Hinder LM, Hayes JM, Backus C, Pennathur S, Kretzler M, Brosius FC, Feldman EL, 2015 The metabolic syndrome and microvascular complications in a murine model of type 2 diabetes. Diabetes, db150133.

Hur J, Sullivan KA, Pande M, Hong Y, Sima AA, Jagadish HV, Kretzler M, Feldman EL, 2011 The identification of gene expression profiles associated with progression of human diabetic neuropathy. Brain 134, 3222–3235. [PubMed: 21926103]

Jia L, Vianna CR, Fukuda M, Berglund ED, Liu C, Tao C, Sun K, Liu T, Harper MJ, Lee CE, 2014 Hepatocyte Toll-like receptor 4 regulates obesity-induced inflammation and insulin resistance. Nature communications 5.

Jung UJ, Choi M-S, 2014 Obesity and its metabolic complications: the role of adipokines and the relationship between obesity, inflammation, insulin resistance, dyslipidemia and nonalcoholic fatty liver disease. International journal of molecular sciences 15, 6184–6223. [PubMed: 24733068]

Kim SJ, Kim HM, 2017 Dynamic lipopolysaccharide transfer cascade to TLR4/MD2 complex via LBP and CD14. BMB reports 50, 55. [PubMed: 28115037]

Koyasu S, 2003 The role of PI3K in immune cells. Nature immunology 4, 313. [PubMed: 12660731]

Le Stunff C, Dechartres A, Mariot V, Lotton C, Trainor C, Del Giudice EM, Meyre D, Bieche I, Laurendeau I, Froguel P, 2008 Association analysis indicates that a variant GATA-binding site in the PIK3CB promoter is a Cis-acting expression quantitative trait locus for this gene and attenuates insulin resistance in obese children. Diabetes 57, 494–502. [PubMed: 17977952]

Lee JH, Cox DJ, Mook DG, McCarty RC, 1990 Effect of hyperglycemia on pain threshold in alloxan-diabetic rats. Pain 40, 105–107. [PubMed: 2339005]

Lee JY, Zhao L, Youn HS, Weatherill AR, Tapping R, Feng L, Lee WH, Fitzgerald KA, Hwang DH, 2004 Saturated fatty acid activates but polyunsaturated fatty acid inhibits Toll-like receptor 2 dimerized with Toll-like receptor 6 or 1. Journal of Biological Chemistry 279, 16971–16979. [PubMed: 14966134]

Liu X-J, Liu T, Chen G, Wang B, Yu X-L, Yin C, Ji R-R, 2016 TLR signaling adaptor protein MyD88 in primary sensory neurons contributes to persistent inflammatory and neuropathic pain and neuroinflammation. Scientific reports 6, 28188. [PubMed: 27312666]

Lu Y-C, Yeh W-C, Ohashi PS, 2008 LPS/TLR4 signal transduction pathway. Cytokine 42, 145–151. [PubMed: 18304834]

Lumeng CN, 2013 Innate immune activation in obesity. Molecular aspects of medicine 34, 12–29. [PubMed: 23068074]

McGregor BA, Eid S, Rumora AE, Murdock B, Guo K, de Anda-Jáuregui G, Porter JE, Feldman EL, Hur J, 2018 Conserved Transcriptional Signatures in Human and Murine Diabetic Peripheral Neuropathy. Scientific reports 8, 17678. [PubMed: 30518872]

Murdock BJ, Falkowski NR, Shreiner AB, Akha AAS, McDonald RA, White ES, Toews GB, Huffnagle GB, 2012 Interleukin-17 drives pulmonary eosinophilia following repeated exposure to Aspergillus fumigatus conidia. Infection and immunity 80, 1424–1436. [PubMed: 22252873]

O'Brien PD, Hinder LM, Rumora AE, Hayes JM, Dauch JR, Backus C, Mendelson FE, Feldman EL, 2018 Juvenile murine models of prediabetes and type 2 diabetes develop neuropathy. Disease models & mechanisms 11, dmm037374. [PubMed: 30446513]

O'Brien PD, Hur J, Hayes JM, Backus C, Sakowski SA, Feldman EL, 2015 BTBR ob/ob mice as a novel diabetic neuropathy model: Neurological characterization and gene expression analyses. Neurobiology of disease 73, 348–355. [PubMed: 25447227]

O'Brien PD, Sakowski SA, Feldman EL, 2014 Mouse models of diabetic neuropathy. ILAR journal 54, 259–272. [PubMed: 24615439]

O'Brien PD, Hur J, Robell NJ, Hayes JM, Sakowski SA, Feldman EL, 2016 Gender-specific differences in diabetic neuropathy in BTBR ob/ob mice. Journal of Diabetes and its Complications 30, 30–37. [PubMed: 26525588]

Obrosova IG, Ilnytska O, Lyzogubov VV, Pavlov IA, Mashtalir N, Nadler JL, Drel VR, 2007 High-fat diet–induced neuropathy of pre-diabetes and obesity: effects of "healthy" diet and aldose reductase inhibition. Diabetes 56, 2598–2608. [PubMed: 17626889]

Ogden CL, Carroll MD, Kit BK, Flegal KM, 2014 Prevalence of childhood and adult obesity in the United States, 2011–2012. Jama 311, 806–814. [PubMed: 24570244]

Ogurtsova K, da Rocha Fernandes J, Huang Y, Linnenkamp U, Guariguata L, Cho N, Cavan D, Shaw J, Makaroff L, 2017 IDF Diabetes Atlas: Global estimates for the prevalence of diabetes for 2015 and 2040. Diabetes research and clinical practice 128, 40–50. [PubMed: 28437734]

Oh SS, Hayes JM, Sims-Robinson C, Sullivan KA, Feldman EL, 2010 The effects of anesthesia on measures of nerve conduction velocity in male C57Bl6/J mice. Neuroscience letters 483, 127–131. [PubMed: 20691755]

Pande M, Hur J, Hong Y, Backus C, Hayes JM, Oh SS, Kretzler M, Feldman EL, 2011 Transcriptional profiling of diabetic neuropathy in the BKS db/db mouse: a model of type 2 diabetes. Diabetes, DB_101541.

Pop-Busui R, Boulton AJ, Feldman EL, Bril V, Freeman R, Malik RA, Sosenko JM, Ziegler D, 2017 Diabetic neuropathy: a position statement by the American Diabetes Association. Diabetes Care 40, 136–154. [PubMed: 27999003]

Ramesh G, MacLean AG, Philipp MT, 2013 Cytokines and chemokines at the crossroads of neuroinflammation, neurodegeneration, and neuropathic pain. Mediators of inflammation 2013.

Reyna SM, Ghosh S, Tantiwong P, Meka CR, Eagan P, Jenkinson CP, Cersosimo E, DeFronzo RA, Coletta DK, Sriwijitkamol A, 2008 Elevated toll-like receptor 4 expression and signaling in muscle from insulin-resistant subjects. Diabetes 57, 2595–2602. [PubMed: 18633101]

Shi H, Kokoeva MV, Inouye K, Tzameli I, Yin H, Flier JS, 2006 TLR4 links innate immunity and fatty acid–induced insulin resistance. Journal of Clinical Investigation 116, 3015. [PubMed: 17053832]

Song MJ, Kim KH, Yoon JM, Kim JB, 2006 Activation of Toll-like receptor 4 is associated with insulin resistance in adipocytes. Biochemical and biophysical research communications 346, 739–745. [PubMed: 16781673]

Stevens MJ, Dananberg J, Feldman EL, Lattimer SA, Kamijo M, Thomas TP, Shindo H, Sima A, Greene DA, 1994 The linked roles of nitric oxide, aldose reductase and,(Na+, K+)-ATPase in the slowing of nerve conduction in the streptozotocin diabetic rat. The Journal of clinical investigation 94, 853–859. [PubMed: 8040341]

Strauss-Ayali D, Conrad SM, Mosser DM, 2007 Monocyte subpopulations and their differentiation patterns during infection. Journal of leukocyte biology 82, 244–252. [PubMed: 17475785]

Sullivan KA, Hayes JM, Wiggin TD, Backus C, Oh SS, Lentz SI, Brosius F, Feldman EL, 2007 Mouse models of diabetic neuropathy. Neurobiology of disease 28, 276–285. [PubMed: 17804249]

Wiggin TD, Kretzler M, Pennathur S, Sullivan KA, Brosius FC, Feldman EL, 2008 Rosiglitazone treatment reduces diabetic neuropathy in streptozotocin-treated DBA/2J mice. Endocrinology 149, 4928–4937. [PubMed: 18583417]

Wu F.-x., Bian J.-j., Miao X.-r., Huang S.-d., Xu X.-w., Gong D.-j., Sun Y.-m., Lu Z.-j., Yu W.-f., 2010 Intrathecal siRNA against Toll-like receptor 4 reduces nociception in a rat model of neuropathic pain. International journal of medical sciences 7, 251. [PubMed: 20714435]

Yang R-H, Lin J, Hou X-H, Cao R, Yu F, Liu H-Q, Ji A-L, Xu X-N, Zhang L, Wang F, 2014 Effect of docosahexaenoic acid on hippocampal neurons in high-glucose condition: involvement of PI3K/AKT/nuclear factor-κB-mediated inflammatory pathways. Neuroscience 274, 218–228. [PubMed: 24881575]

Zeng J, Xu Y, Shi Y, Jiang C, 2018 Inflammation Role in Sensory Neuropathy in Chinese Patients with Diabetes/Prediabetes. Clinical Neurology and Neurosurgery.

Zhang C, Ward J, Dauch JR, Tanzi RE, Cheng HT, 2018 Cytokine-mediated inflammation mediates painful neuropathy from metabolic syndrome. PloS one 13, e0192333. [PubMed: 29408929]

Zhang Z, Amorosa LF, Coyle SM, Macor MA, Birnbaum MJ, Lee LY, Haimovich B, 2016 Insulin-dependent regulation of mTORC2-Akt-FoxO suppresses TLR4 signaling in human leukocytes: Relevance to type 2 diabetes. Diabetes 65, 2224–2234. [PubMed: 27207509]

Zhu T, Meng Q, Ji J, Lou X, Zhang L, 2015 Toll-like receptor 4 and tumor necrosis factor-alpha as diagnostic biomarkers for diabetic peripheral neuropathy. Neuroscience letters 585, 28–32. [PubMed: 25445373]

Zhuang Z-Y, Xu H, Clapham DE, Ji R-R, 2004 Phosphatidylinositol 3-kinase activates ERK in primary sensory neurons and mediates inflammatory heat hyperalgesia through TRPV1 sensitization. Journal of Neuroscience 24, 8300–8309. [PubMed: 15385613]

Highlights

- Toll-like receptors 2 and 4 play a role in peripheral neuropathy in mouse and man

- Knocking out toll-like receptors 2 and 4 affects neuropathy in mice

- Toll-like receptor signaling varies with disease progression
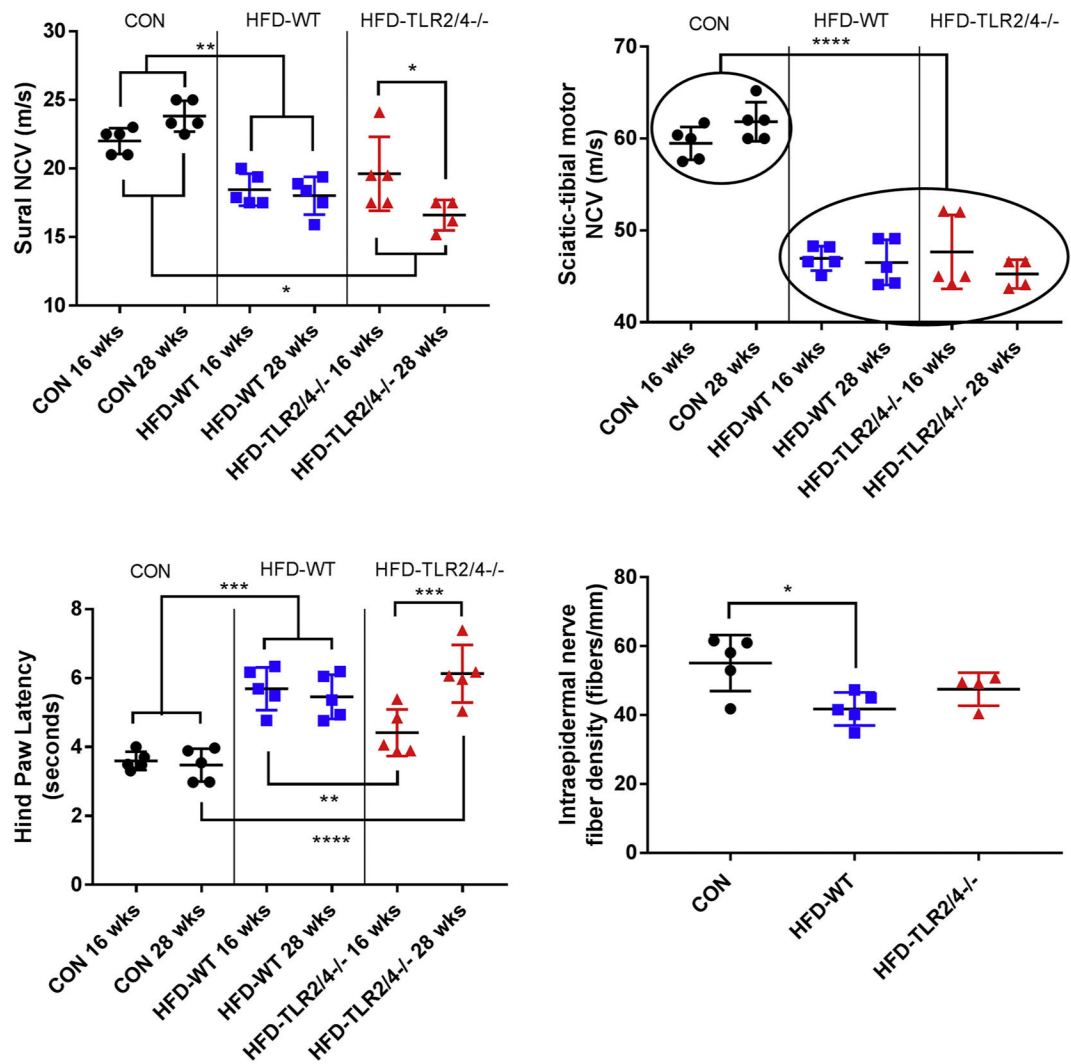
Figure 1.
Neuropathy phenotyping at early and late time points. Nerve conduction velocities (NCV; m/s) of the (A) sural and (B) sciatic-tibular motor nerves in CON (3 males and 2 females), HFD-WT (2 males and 3 females), and HFD-TLR2/4$^{-/-}$ (2 males and 3 females) mice at 16 and 28 wks of age. (C) Hind paw withdrawal latency (HPL) at 16 and 28 wks of age. (D) Intraepidermal nerve fiber density (IENFD) at 28 wks of age. Data are represented as means ± SEM. * P 0.05, ** P 0.01, *** P 0.001, and **** P 0.0001.
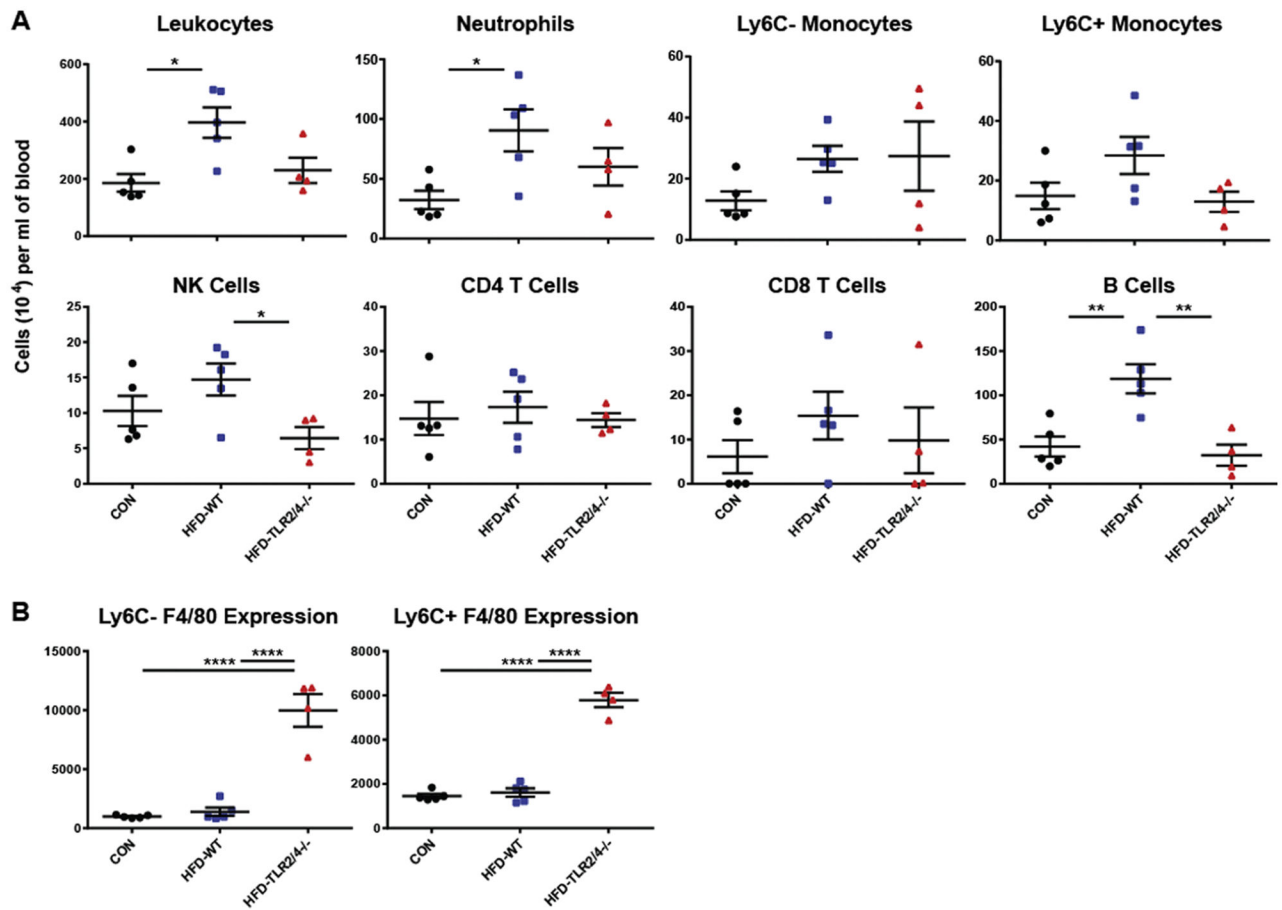
Figure 2.
Peripheral blood leukocyte levels and F4/80 expression at the late time point. CON, HFD-WT, and HFD-TLR2/4$^{-/-}$ mice were sacrificed at 28 wks of age, and leukocyte levels in the peripheral blood were assessed using flow cytometry (A), as was F4/80 surface expression on Ly6C− and Ly6C+ monocytes (B). Data are represented as means ± SEM. * P 0.05, ** P 0.01, and **** P 0.0001.

Table 1.

Significantly altered TLR2/4 related gene expression in human sural nerves.

| Gene ID	Gene Symbol	Gene Description	ChipInspector	+ GenePattern
208	AKT2	v-akt murine thymoma viral oncogene homolog 2	−1.12	
841	CASP8	caspase 8, apoptosis-related cysteine peptidase	−1.08	
942	CD86	CD86 molecule	1.21	
6373	CXCL11	chemokine (C-X-C motif) ligand 11	−1.17	
4283	CXCL9	chemokine (C-X-C motif) ligand 9	−1.33	
2353	FOS	FBJ murine osteosarcoma viral oncogene homolog	1.46	
3454	IFNAR1	interferon (alpha, beta and omega) receptor 1	1.15	
3455	IFNAR2	interferon (alpha, beta and omega) receptor 2	−1.1	
3663	IRF5	interferon regulatory factor 5	−1.14	
3725	JUN	jun proto-oncogene	1.16	1.14
3929	LBP	lipopolysaccharide binding protein	−1.31	−1.59
5604	MAP2K1	mitogen-activated protein kinase kinase 1	−1.14	
5609	MAP2K7	mitogen-activated protein kinase kinase 7	1.12	
6885	MAP3K7	mitogen-activated protein kinase kinase kinase 7	−1.09	
1326	MAP3K8	mitogen-activated protein kinase kinase kinase 8	−1.16	
5594	MAPK1	mitogen-activated protein kinase 1	1.15	
5602	MAPK10	mitogen-activated protein kinase 10	−1.13	
1432	MAPK14	mitogen-activated protein kinase 14	−1.12	
5599	MAPK8	mitogen-activated protein kinase 8	−1.08	
5291	PIK3CB	phosphoinositide-3-kinase, catalytic, beta polypeptide	−1.14	−1.4
5294	PIK3CG	phosphoinositide-3-kinase, catalytic, gamma polypeptide	−1.1	
5295	PIK3R1	phosphoinositide-3-kinase, regulatory subunit 1 (alpha)	1.18	
5296	PIK3R2	phosphoinositide-3-kinase, regulatory subunit 2 (beta)	1.09	
8503	PIK3R3	phosphoinositide-3-kinase, regulatory subunit 3 (gamma)	−1.12	
6772	STAT1	signal transducer and activator of transcription 1, 91kDa	−1.14	
23118	TAB2	TGF-beta activated kinase 1/MAP3K7 binding protein 2	1.11	
148022	TICAM1	toll-like receptor adaptor molecule 1	1.16	1.16

Previously published data (Hur et al., 2011) represented as relative fold changes in sural nerve gene expression between neuropathy patients who either worsened in their neuropathy (progressors) or had no change in neuropathy (non-progressors), with non-progressors used as the reference set for the two different analyses (ChipInspector and ChipInspector + GenePattern).

Table 2.

TLR2/4 gene expression in murine sural nerves using RNAseq or microarray profiling

Gene ID	Gene Symbol	Gene Description	db/+ vs db/db (8 wk (Hinder et al., 2018))	db/+ vs db/db (24 wk (Pande et al., 2011))	8wk vs 24 wk (db/db (Hinder et al., 2018))	Con vs Diabetic (26 wk (Wiggin et al., 2008))	db/+ vs db/db (16 wk (Hur et al., 2015))	db/db vs tx (16 wk (Hur et al., 2015))	ob/+ vs ob/ob (26 wk (O'Brien et al., 2016))	ob/+ vs ob/ob (5 wk (O'Brien et al., 2015))	5 wk vs 13 wk (ob/ob (O'Brien et al., 2015))	Con vs db/db (16 wk (Hinder et al., 2017b))	db/db vs tx (16 wk (Hinder et al., 2017b))
11651	Akt1	thymoma viral proto-oncogene 1						-1.18					
11652	Akt2	thymoma viral proto-oncogene 2					-1.38	1.7					1.22
23797	Akt3	thymoma viral proto-oncogene 3	-1.51	-1.78				-1.47			-1.16		
12370	Casp8	caspase 8		1.91	1.91			1.68					
20293	Ccl12	chemokine (C-C motif) ligand 12				-1.78		2.59					
20302	Ccl3	chemokine (C-C motif) ligand 3		4.47		-1.68				3.57	-3.32	3.98	
20303	Ccl4	chemokine (C-C motif) ligand 4		2.94						1.55	-1.36		
20304	Ccl5	chemokine (C-C motif) ligand 5							3.2			4.12	
12475	Cd14	CD14 antigen					1.46			2.26	-1.54		
21939	Cd40	CD40 antigen						1.6				2.09	
12524	Cd86	CD86 antigen			-1.69						-1.65		
12675	Chuk	conserved helix-loop-helix ubiquitous kinase	1.2	1.34									
15945	Cxcl10	chemokine (C-X-C motif) ligand 10		7.2									
17329	Cxcl9	chemokine (C-X-C motif) ligand 9		1.84			-1.99	11.06					
14082	Fadd	Fas (TNFRSF6)-associated via death domain				1.85							
15975	Ifnar1	interferon (alpha and beta) receptor 1						-1.24					-1.17
15976	Ifnar2	interferon (alpha and beta) receptor 2		1.39									
56489	Ikbke	inhibitor of kappaB kinase epsilon						-1.31				1.61	
16151	Ikbkg	inhibitor of kappaB kinase gamma	1.43				-1.23	1.16					
16176	Il1b	interleukin 1 beta								4.45	-4.62		
54131	Irf3	interferon regulatory factor 3			-1.39								
27056	Irf5	interferon regulatory factor 5		1.7						1.46		2.39	
54123	Irf7	interferon regulatory factor 7	-2.24			2.07	-1.69						
16476	Jun	Jun oncogene		-1.44									

Gene ID	Gene Symbol	Gene Description	db/+ vs db/db (8 wk (Hinder et al., 2018))	db/+ vs db/db (24 wk (Pande et al., 2011))	8wk vs 24 wk (db/db) (Hinder et al., 2018))	Con vs Diabetic (26 wk (Wiggin et al., 2008))	db/+ vs db/db (16 wk (Hur et al., 2015))	db/db vs tx (16 wk (Hur et al., 2015))	ob/+ vs ob/ob (26 wk (O'Brien et al., 2016))	ob/+ vs ob/ob (5 wk (O'Brien et al., 2015))	5 wk vs 13 wk (ob/ob (O'Brien et al., 2015))	Con vs db/db (16 wk (Hinder et al., 2017b))	db/db vs tx (16 wk (Hinder et al., 2017b))
16803	Lbp	lipopolysaccharide binding protein	1.73	1.81	−1.38	1.48		−1.27		1.44			
17087	Ly96	lymphocyte antigen 96						1.37					
26395	Map2k1	mitogen-activated protein kinase kinase 1			1.27								
26397	Map2k3	mitogen-activated protein kinase kinase 3		1.46				1.33					
26398	Map2k4	mitogen-activated protein kinase kinase 4	1.19										
26399	Map2k6	mitogen-activated protein kinase kinase 6						−1.32					
26400	Map2k7	mitogen-activated protein kinase kinase 7						−1.24			1.3		
26410	Map3k8	mitogen-activated protein kinase kinase kinase 8		1.5			1.63						
26413	Mapk1	mitogen-activated protein kinase 1									−1.28		
26414	Mapk10	mitogen-activated protein kinase 10		−15.96				−1.76					
29857	Mapk12	mitogen-activated protein kinase 12	−1.58	−1.51		1.55							−1.24
26417	Mapk3	mitogen-activated protein kinase 3											
26420	Mapk9	mitogen-activated protein kinase 9									1.18		
18035	Nfkbia	nuclear factor of kappa light polypeptide gene enhancer in B-cells inhibitor, alpha			−1.48					1.28			
18706	Pik3ca	phosphatidylinositol 3-kinase, catalytic, alpha polypeptide									1.23		
74769	Pik3cb	phosphatidylinositol 3-kinase, catalytic, beta polypeptide	1.89	1.73				1.77				1.38	
18709	Pik3r2	phosphatidylinositol 3-kinase, regulatory subunit, polypeptide 2 (p85 beta)	−1.53		−1.44			−1.47					
18710	Pik3r3	phosphatidylinositol 3 kinase, regulatory subunit, polypeptide 3 (p55)	1.43		1.47		1.3						
320207	Pik3r5	phosphoinositide-3-kinase, regulatory subunit 5, p101	1.78	3.05			1.98		2.62	1.87		4.32	

Gene ID	Gene Symbol	Gene Description	db/+ vs db/db (8 wk (Hinder et al., 2018))	db/+ vs db/db (24 wk (Pande et al., 2011))	8wk vs 24 wk (db/db (Hinder et al., 2018))	Con vs Diabetic (26 wk (Wiggin et al., 2008))	db/+ vs db/db (16 wk (Hur et al., 2015))	db/db vs tx (16 wk (Hur et al., 2015))	ob/+ vs ob/ob (26 wk (O'Brien et al., 2016))	ob/+ vs ob/ob (5 wk (O'Brien et al., 2015))	5 wk vs 13 wk (ob/ob (O'Brien et al., 2015))	Con vs db/db (16 wk (Hinder et al., 2017b))	db/db vs tx (16 wk (Hinder et al., 2017b))
19697	Rela	v-rel reticuloendotheliosis viral oncogene homolog A (avian)						−1.15					
19766	Ripk1	receptor (TNFRSF)-interacting serine-threonine kinase 1		1.36									
20750	Spp1	secreted phosphoprotein 1				−1.32	−1.26			1.53		−2.13	
20846	Stat1	signal transducer and activator of transcription 1					−1.35						
66513	Tab1	TGF-beta activated kinase 1/ MAP3K7 binding protein 1	−1.3					−1.28				1.26	−1.23
68652	Tab2	TGF-beta activated kinase 1/ MAP3K7 binding protein 2						−1.27					
56480	Tbk1	TANK-binding kinase 1					1.27			1.23		1.28	
106759	Ticam1	toll-like receptor adaptor molecule 1						−1.28					
24088	Tlr2	toll-like receptor 2								1.34	−1.52		
21926	Tnf	tumor necrosis factor		2.06						1.47			
54473	Tollip	toll interacting protein			1.12								
22031	Traf3	TNF receptor-associated factor 3		1.45									

Previously published data (Hinder et al., 2017b; Hur et al., 2015; O'Brien et al., 2015; O'Brien et al., 2016; Pande et al., 2011; Wiggin et al., 2008) represented as relative fold changes in sural nerve gene expression across murine models of neuropathy. Con=control and tx=treated. The group listed first is the group used as reference.

Table 3.

TLR2/4 DEGs across human and murine tissue

Significant Human DEGs	Number of Mouse Models with Significant DEGs	Direction of Human Dysregulation	Direction of Mouse Dysregulation		
			Diabetic vs control	Changes over time	Diabetic in response to treatment
AKT2	3	↓	↓		↑
CASP8	3	↓	↑	↑	↑
CD86	3	↑	↑	↓	
CXCL9	3	↓	↔		↑
IFNAR1	2	↑			↓
IFNAR2	1	↓	↑		
IRF5	3	↓	↑		
JUN	1	↑	↓		
LBP	6	↓	↑	↓	↓
MAP2K1	1	↓		↑	
MAP2K7	2	↑		↑	↓
MAP3K8	2	↓	↑		
MAPK1	1	↑		↓	
MAPK10	2	↓	↓		↓
PIK3CB	4	↓	↑		↑
PIK3R2	3	↑	↓	↓	↓
PIK3R3	3	↓	↑	↑	
STAT1	1	↓	↓		
TAB2	1	↑			↓
TICAM1	1	↑			↓

Significantly dysregulated genes in both human and murine neuropathy and their directionality. Cells highlighted in blue represent downregulated gene expression, red represent upregulated gene expression, and purple represent mixed directionality of gene expression. Cells highlighted in green in the 'Significant Human DEGs' column represent significantly dysregulated genes using both ChipInspector and ChipInspector + GenePattern analysis platforms in the human data, and cells highlighted in green in the 'Number of Mouse Models with Significant DEGs' column represent significantly dysregulated genes across both human analysis platforms and across 4 or more mouse models.

Table 4.

Late stage body weights and fasting blood glucose in CON (3 males and 2 females), HFD-WT (2 males and 3 females), and HFD-TLR2/4$^{-/-}$ (2 males and 3 females) mice.

Body weight and fasting blood glucose	CON (n=5)	HFD-WT (n=5)	HFD-TLR2/4$^{-/-}$ (n=5)
Weight (g)	27.8 ± 3.5	48.4 ± 3.5[*]	57.4 ± 3.5[*]
Fasting blood glucose (mg/dL)	146.4 ± 13.0	196.3 ± 13.0	172.3 ± 14.3

Data are represented as least square means ± SEM.

[*] indicates a $P < 0.05$ difference from CON.